the GFR change under stimulate conditions. The $k_2 \cdot p_{phys}$ value in cortical region obtained in the present study was 3.64 ± 2.15 ml/min/g under the normal condition and showed similar value to literature normal of 4 to 5 ml/min/g [22]. In comparison to Middlekauff et al [23-25], they applied the ROI base analysis, showing similar RBF values around 4 ml/min/g. These findings also supports to apply the $k_2 \cdot p_{phys}$ as RBF. The different values in RBF between the present results and the previous ones [3-5] might be due to the difference of approach.

The present computation for RBF applied BFM, which has two main advantages over the nonlinear NLF. One is the ability to produce a voxel-by-voxel quantitative parametric map, and the other is faster computing speed. In fact, the parametric images were obtained within reasonable time, i.e., two min and half with image size of 128 × 128 pixels with 35 slices and 22 frames. It could be further reduced by applying a threshold to omit pixel with lower values. For a clinical stand point, voxel-by-voxel analysis is preferred to ROI-based analysis because the operator can independently define ROIs to improve reproducibility, and faster computations are important for analyzing enormous datasets.

Kinetic parameters estimated by the NLF agreed well with those estimated by the BFM as shown in Fig 2. The disagreement in some rate constant values between the voxel-based (BFM) and ROI based computation methods might be due to composite structure between cortical region and surroundings or image noise. Although superior to the NLF in terms of computing speed and ability to generate parametric maps, the BFM shares the same source of errors as the NLF because they use the same model and assumption. Delay and dispersion in input function, motion of a patient during a study [26-28], and flow heterogeneity [29], are sources of error for parameters estimated by both the NLF and BFM. Selection of specific range of k_2 and the number of basis function can affect accuracy and precision of estimated parameters in neuroreceptor studies [30, 31]. However, the lower and upper limit on that range was 0 and 15 ml/min/g in the present computation with $H_2{}^{15}O$ and

this limit would be enough for the present computation. In practice, selection of wider range and/or large number of discrete values of basis function is slow and inefficient against required accuracy and precision.

The present simulation study showed that if V_A is neglected or fixed, not only the absolute rate constants, i.e. RBF value is overestimated, but estimated changes in RBF between two physiological states could be over- or underestimated. These findings suggest that V_A should be included to obtain either absolute or relative value of RBF. For p, the present simulation revealed that the error sensitivity in RBF on that value was significant. The present experimental data showed that the values of p for whole and cortical regions were 0.35 and 0.42 ml/g, respectively. If the value was fixed to 0.4 ml/g, a 40 % overestimation in RBF for regions with p of 0.35 occurred, thus, regional difference of p introduces error in quantitative RBF values. Also AIC analysis showed that introducing those extra parameters of p and V_A did not increase the AIC value against others. These findings suggest that both p and V_A need to be estimated simultaneously with quantitative RBF, especially when changes on different conditions are assessed.

The knowledge of RBF is mostly needed in determining the severity of renovascular disease. Though the degree of renal arterial stenosis is easily diagnosed, its actual effect on RBF remains difficult to quantify. In clinical work, estimates of GFR have not shown very good accuracy to a possible interventional treatment. Also, there is no good clinical method to easily measure single kidney or regional RBF. We can obtain the effective renal plasma flow (ERPF) by infusing p-aminohippuric acid and measuring their urine and plasma concentrations, but this method only gives the total ERPF for both kidneys. Alternative is magnetic resonance (MR) based method, which is problematic in patients with chronic kidney disease, because the contrast agent gadolinium is contraindicated in these subjects [32]. The present PET-related methodology may provide quantitative regional RBF, and be clinically

applicable in conditions such as chronic allograft nephropathy and acute kidney insufficiency. The procedure – as presented here – still implies a small degree of invasiveness because of blood sampling. However, many non-invasive methods for estimating input functions have been proposed [3-5, 23-25, 33, 34], and their implementation will allow to examine RBF in a fully non-invasive fashion, particularly for clinical purposes.

In conclusion, although some issues remain to be investigated, this study shows the feasibility of measurement of RBF using PET with $H_2{}^{15}O$.

Acknowledgments

The authors thank the technical staff of the Turku PET Centre for the efforts and skills dedicated to this project. This work is supported by the Hospital District of Southwest of Finland and was conducted within the "Centre of Excellence in Molecular Imaging in Cardiovascular and Metabolic Research" supported by the Academy of Finland, University of Turku, Turku University Hospital and Abo Academy. The study was further supported by grants from the Academy of Finland (206359 to P.N.), Finnish Diabetes Foundation (P.I.), EFSD/Eli-Lilly (P.I.), Sigrid Juselius Foundation (N.K. and P.I.), and Novo Nordisk Foundation (P.N.).

References

1. Nitzsche EU, Choi Y, Killion D, Hoh CK, Hawkins RA, Rosenthal JT, Buxton DB, Huang SC, Phelps ME, Schelbert HR. Quantification and parametric imaging of renal cortical blood flow in vivo based on Patlak graphical analysis. Kidney Int. 1993; 44:985-996.

2. Szabo Z, Xia J, Mathews WB, Brown PR. Future direction of renal positron emission tomography. Semin Nucl Med. 2006; 36:36-50.

3. Juillard L, Janier MF, Foucue D, Lionnet M, Le Bars D, Cinotti L, Barthez P, Gharib C, Laville M. Renal blood flow measurement by positron emission tomography using ^{15}O-labeled water. Kidney Int. 2000; 57: 2511-2518.

4. Juillard L, Janier MF, Fouque D, Cinotti L, Maakel N, Le Bars D, Barthez PY, Pozet N, Laville M. Dynamic renal blood flow measurement by positron emission tomography in patients with CRF. Am. J. Kidney Dis. 2002; 40:947-954.

5. Alpert NM, Rabito CA, Correia DJA, Babich JW, Littman BH, Tompkins RG, Rubin NT, Rubin RH, Fischman AJ. Mapping of local renal blood flow with PET and $H_2{}^{15}O$. J. Nucl. Med. 2002; 43: 470-475.

6. Anderson HL, Yap JT, Miller MP, Robbins A, Jones T, Price PM. Assessment of pharmacodynamic vascular response in a phase I trial of combretastatin A4 phosphate. J. Clin. Oncol. 2003; 21: 2823-2830.

7. Anderson H, Yap JT, Wells P, Miller MP, Propper D, Price D, Harris AL. Measurement of renal tumour and normal tissue perfusion using positron emission tomography in a phase II clinical trial of razoxane. Br. J. Cancer 2003; 89: 262-267.

8. WC Snyder, MJ Cook, ES Nasset LR Karhausen G Parry Howells IH Tipton Report of the Task Group on Reference Man. Pergamon Press 1974; pp. 175-177.

9. Herscovitch P, Raichle ME What is the correct value for the brain--blood partition coefficient for water? J Cereb Blood Flow Metab. 1985; 5: 65-9.

10. Iida H, Law I, Pakkenberg B, Krarup-Hansen A, Eberl S, Holm S, Hansen AK, Gundersen HJ, Thomsen C, Svarer C, Ring P, Friberg L, Paulson OB Quantitation of regional cerebral blood flow corrected for partial volume effect using O-15 water and PET: I. Theory, error analysis, and stereologic comparison. J Cereb Blood Flow Metab 2000; 20:1237-1251

11. G. Blomqvist, A.A. Lammertsma, B. Mazoyer, K. Wienhard Effect of tissue heterogeneity on quantification in positron emission tomography. European Journal of Nuclear Medicine (1995) 22:652-663

12. Koeppe RA, Holden JE, Ip WR Performance comparison of parameter estimation techniques for the quantitation of local cerebral blood flow by dynamic positron computed tomography. J Cereb Blood Flow Metab. 1985; 5: 224-34.

13. Gunn RN, Lammertsma AA, Hume SP, et al. Parametric imaging of ligand-receptor binding in PET using a simplified reference region model. Neuroimage. 1997; 6: 279–287

14. Watabe H, Jino H, Kawachi N, Teramoto N, Hayashi T, Ohta Y, Iida H. Parametric imaging of myocardial blood flow with 15O-water and PET using the basis function method. J Nucl Med. 2005; 46: 1219-24.

15. Boellaard R, Knaapen P, Rijbroek A, Luurtsema GJ, Lammertsma AA. Evaluation of basis function and linear least squares methods for generating parametric blood flow images using ^{15}O-water and Positron Emission Tomography. Mol Imaging Biol. 2005; 7: 273-85.

16. Ruotsalainen U, Raitakari M, Nuutila P, Oikonen V, Sipilä H, Teräs M, Knuuti MJ, Bloomfield PM, Iida H. Quantitative blood flow measurement of skeletal muscle using oxygen-15-water and PET. J Nucl Med 1997; 38: 314-9

17. Levey A, Bosch J, Lewis J, et al. A more accurate method to estimate glomerular filtration rate from serum creatinine: a new prediction equation. Modification of Diet in Renal Disease Study Group. Ann Intern Med 1999; 130:461-70

18. Iida H, Kanno I, Miura S, Murakami M, Takahashi K, Uemura K. Error analysis of a quantitative cerebral blood flow measurement using $H_2{}^{15}O$ autoradiography and positron emission tomography, with respect to the dispersion of the input function J, Cereb Blood Flow Metab 1986; 6: 536-45

19. Iida H, Higano S, Tomura N, Shishido F, Kanno I, Miura S, Murakami M, Takahashi K, Sasaki H, Uemura K Evaluation of regional differences of tracer appearance time in cerebral tissues using [^{15}O] water and dynamic positron emission tomography. J Cereb Blood Flow Metab 1988; 8: 285-288

20. Akaike H. A new look at the statistical model identification. IEEE Trans Automat Contr. 1974;AC19:716–723.

21. Kudomi N, Hayashi T, Teramoto N, Watabe H, Kawachi N, Ohta Y, Kim KM, Iida H. Rapid quantitative measurement of $CMRO_2$ and CBF by dual administration of ^{15}O-labeled oxygen and water during a single PET scan-a validation study and error analysis in anesthetized monkeys. J Cereb Blood Flow Metab. 2005; 259: 1209-24.

22. Ganong WF Review of Medical Physiology. 8th edition LANGE Medical Publications, 1977; pp. 522-545

23. Middlekauff HR, Nitzsche EU, Hamilton MA, Schelbert HR, Fonarow GC, Moriguchi JD, Hage A, Saleh S, Gibbs GG. Evidence for preserved cardiopulmonary baroflex control of renal cortical blood flow in humans with advanced heart failure. Circulation 1995; 92: 395-401.

24. Middlekauff HR, Nitzsche EU, Hoh CK, Hamilton MA, Fonarow GC, Hage A, Moriguchi JD. Exaggerated renal vasoconstriction during exercise in heart failure patients. Circulation 2000; 101: 784-789.

25. Middlekauff HR, Nitzsche EU, Hoh CK, Hamilton MA, Fonarow GC, Hage A, Moriguchi JD. Exaggerated muscle mechanoreflex control of reflex renal vasoconstriction in heart failure. J. Appl. Physiol. 2001; 90: 1714-1719.

26. Fulton RR, Meikle SR, Eberl S, et al. Correction for head movements in positron emission tomography using an optical motion-tracking system. IEEE Trans Nucl Sci. 2002; 49:116–123

27. Bloomfield PM, Spinks TJ, Reed J, et al. The design and implementation of a motion correction scheme for neurological PET. Phys Med Biol. 2003; 48: 959–978

28. Woo SK, Watabe H, Choi Y, et al. Sinogram-based motion correction of PET images using optical motion tracking system and list-mode data acquisition. IEEE Trans Nucl Sci. 2004; 51: 782–788.

29. Herrero P, Staudenherz A, Walsh JF, et al. Heterogeneity of myocardial perfusion provides the physiological basis of perfusable tissue index. J Nucl Med. 1995; 36: 320–327

30. Cselényi Z, Olsson H, Halldin C, Gulyás B, Farde L. A comparison of recent parametric neuroreceptor mapping approaches based on measurements with the high affinity PET radioligands [^{11}C]FLB 457 and [^{11}C]WAY 100635. Neuroimage. 2006; 32: 1690-708.

31. Schuitemaker A, van Berckel BN, Kropholler MA, Kloet RW, Jonker C, Scheltens P, Lammertsma AA, Boellaard R. Evaluation of methods for generating parametric (R-[11C]PK11195 binding images. J Cereb Blood Flow Metab. 2007; 27: 1603-15.

32. Martin D, Sharma P, Salman K, et al. Individual kidney blood flow measured with contrast-enhanced first-pass perfusion MR imaging. Radiology 2008; 246:241-8

33. Iida H, Kanno I, Takahashi A, et al. Measurement of absolute myocardial blood flow with $H_2{}^{15}O$ and dynamic positron-emission tomography strategy for quantification in relation to the partial-volume effect. Circulation. 1988; 78:104–115

34. Germano G, Chen BC, Huang S-C, Gambhir SS, Hoffman EJ, Phelps ME. Use of the abdominal aorta for arterial input function determination in the hepatic and renal PET studies. J. Nucl. Med. 1992; 33: 613-620.

Table 1: Baseline characteristics of the present six subjects

	mean ± SD
Age	58 ± 5
P-Kreatinine umol/l	85 ± 10
eGFR ml/min	78 ± 4
Weight kg	82.8 ± 4.5
BMI	26.6 ± 2.2
BP systolic mmHg	136 ± 11
BP diastolic mmHg	82 ± 4
HR min^{-1}	57 ± 5
fP-Chol mmol/l	5.3 ± 1.0
fP-HDL mmol/l	1.5 ± 0.4
fP-Tg mmol/l	1.2 ± 0.4
fP-LDL mmol/l	3.2 ± 0.8
B-Hb g/l	144 ± 12
fP-gluk mmol/l	5.4 ± 0.4

eGFR: estimated glomerular filtration rate according to MDRD study equation

BMI: body mass index

BP: blood pressure

HR: heart rate

fP-Chol: fasting plasma total cholesterol

fP-HDL: fasting plasma high density cholesterol

fP-LDL: fasting plasm low density cholesterol

fP-Tg: fasting plasma triglyserides

B-Hb: blood haemoglobin

fP-gluk: fasting plasma glucose

Table 2: AIC values for the models.

Subject	3-Parameters	p-fixed	V_A-fixed (0.15)	V_A-ignored
1	484. ± 20.	519. ± 28.	499. ± 15.	494. ± 15.
2	474. ± 9.	486. ± 14.	474. ± 9.	477. ± 8.
3	525. ± 12.	523. ± 8.3.	527. ± 10.	527. ± 7.
4	483. ± 14.	497. ± 21.	501. ± 12.	506. ± 13.
5	497. ± 18.	502. ± 19.	508. ± 32.	499. ± 13.
6	496. ± 11.	507. ± 14.	500. ± 9.	497. ± 9.

3-Parameters: Three parameters of K_1 and k_2, V_A were computed, p-fixed: K_1 and V_A was computed with fixing k_2 so as to p=K_1/k_2 =0.35 ml/g, V_A-fixed: K_1 and k_2 were computed with fixing V_A at 0.15 ml/g, V_A-ignored: K_1 and k_2 were computed without taking into account V_A.

Table 3: Values of K_1, $k2 \cdot p_{phys}$ and V_A (n=6) in whole and cortical region calculated by the present method for baseline and enalapril administrated conditions.

	K_1 (ml/min/g)	$k_2 \cdot p_{phys}$ (ml/min/g)	V_A (ml/ml)	GFR (ml/min/g)
Whole region				
Baseline	1.09 ± 0.33	3.11 ± 1.48	0.15 ± 0.09	0.35 ± 2 #
Enalapril	1.03 ± 0.44	2.55 ± 1.29	0.16 ± 0.14	
Cortical region				
Baseline	1.57 ± 0.60*	3.64 ± 2.15*	0.18 ± 0.12*	
Enalapril	1.42 ± 0.39*	3.55 ± 1.64*	0.25 ± 0.14*	

No significant difference was found between baseline and stimulated conditions. * Difference was significant between whole and cortical regions. # kidney weight of 300 g and cortex ratio of 70 % were assumed.

Figure Captions:

Fig. 1: Schematic diagram of the presnet computation procedure by the basis function method (BFM).

Fig. 2: Relationships of the regional ROI values of (A) K_1, (B) k_2 and (C) RBV by ROI based non-linear fitting method and pixel based BFM. The regression lines were, $K_{1,BFM}$ = 0.93 $K_{1,NLF}$ -0.11 ml/min/g (r = 0.80, P< 0.001), $k_{2,BFM}$ = 0.96 $k_{2,NLF}$ -0.13 ml/min/g (r = 0.77, P< 0.001) and $V_{A,BFM}$ = 0.92 $V_{A,NLF}$ -0.00 ml/ml (r = 0.97, P< 0.001), for K_1, k_2 and V_A, respectively.

Fig 3: Fitted curves to measured tissue TAC (plot) by the different computation methods. 3-Parameters: Three parameters of K_1, k_2 and V_A were computed, p-fixed: K_1 and V_A were computed with fixing $p(=K_1/k_2)$ at 0.35 ml/g, V_A-fixed: K_1 and k_2 were computed with fixing V_A at 0.15 ml/g, V_A-ignored: K_1 and k_2 were computed without taking into account V_A.

Fig. 4: Representative parametric images of K_1 (right) and $k2 \cdot p_{phys}$ (left) for one subject under the baseline condition. Coronal (upper) and transverse (lower) views are shown.

Fig. 5: Error propagation from the error in input delay time (a) and dispersion time constant (b) to K_1 and k_2 (two lines were identical). Positive and negative values of error indicate over- and under-correction of delay time and dispersion time, respectively.

Fig. 6: Error propagation from the partition coefficient (p ml/g) to K_1 and k_2. When the true p was varied between 0.6 and 0.8 ml/g, the size of error in RBF was simulated assuming p=0.7 ml/g.

Fig. 7: (a) Error propagation from the arterial blood volume (V_A ml/ml) to K_1 and k_2 (two lines were identical). When the true V_A changed from 0.0 to 0.4 ml/ml, the size of error in the K_1 and k_2 calculated, assuming V_A =0.0 ml/ml, was simulated. (b) Error propagation from the change of arterial blood volume from 0.14 ml/ml (ΔV_A) to the change in K_1 and k_2 from the initial condition (ΔK_1 and Δk_2 ml/min/g) (two lines were identical).

Figure 1

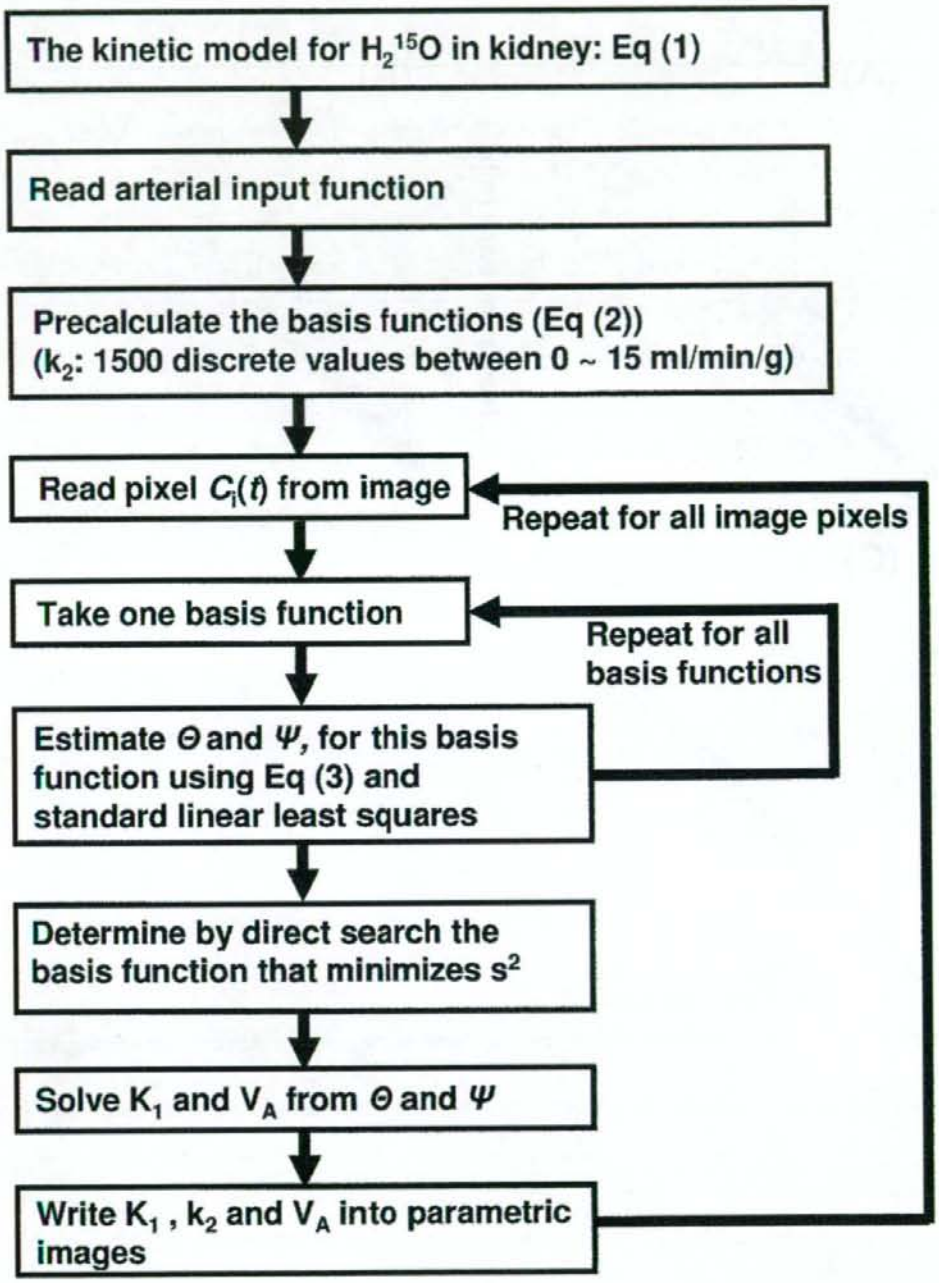
The kinetic model for $H_2{}^{15}O$ in kidney: Eq (1)
Read arterial input function
Precalculate the basis functions (Eq (2))
(k_2: 1500 discrete values between 0 ~ 15 ml/min/g)
Read pixel $C_i(t)$ from image
Repeat for all image pixels
Take one basis function
Repeat for all basis functions
Estimate Θ and Ψ, for this basis function using Eq (3) and standard linear least squares
Determine by direct search the basis function that minimizes s^2
Solve K_1 and V_A from Θ and Ψ
Write K_1 , k_2 and V_A into parametric images

Figure 2

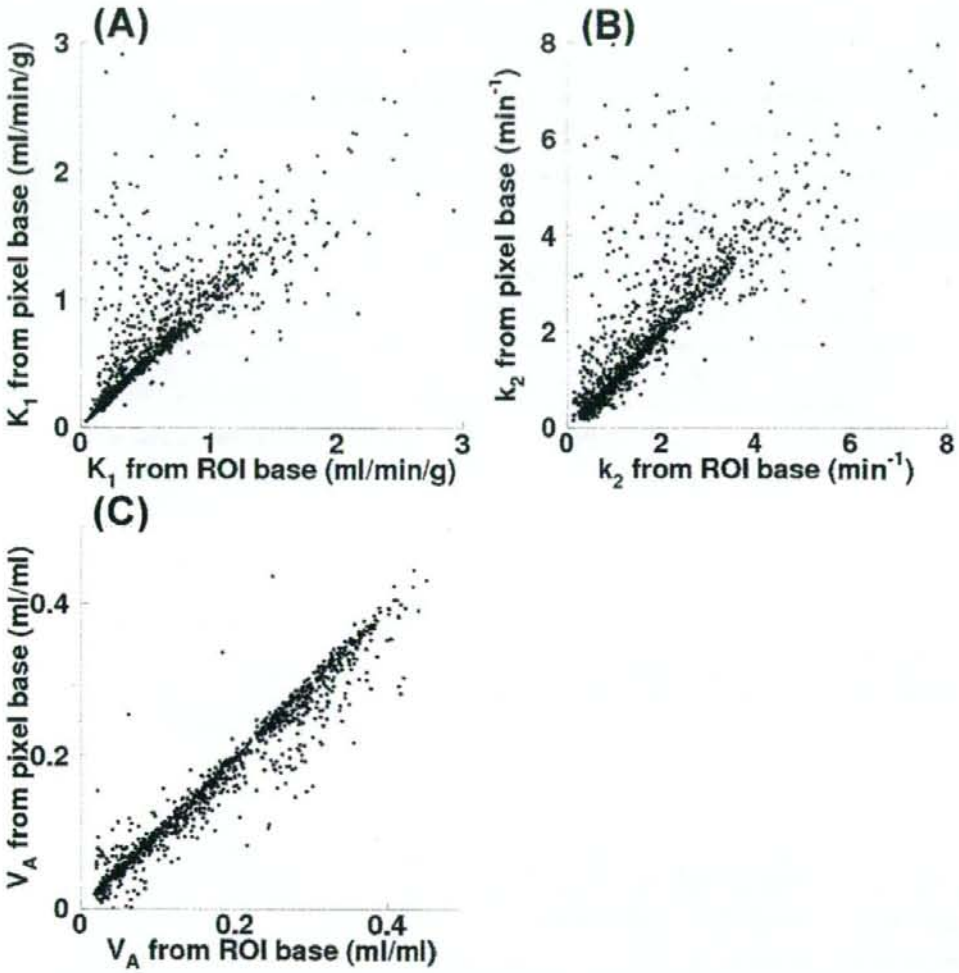
(A)
K1 from pixel base (ml/min/g)
K1 from ROI base (ml/min/g)
0
1
2
3
(B)
k2 from pixel base (min-1)
k2 from ROI base (min-1)
0
2
4
6
8
(C)
VA from pixel base (ml/ml)
VA from ROI base (ml/ml)
0
0.2
0.4

Figure 3

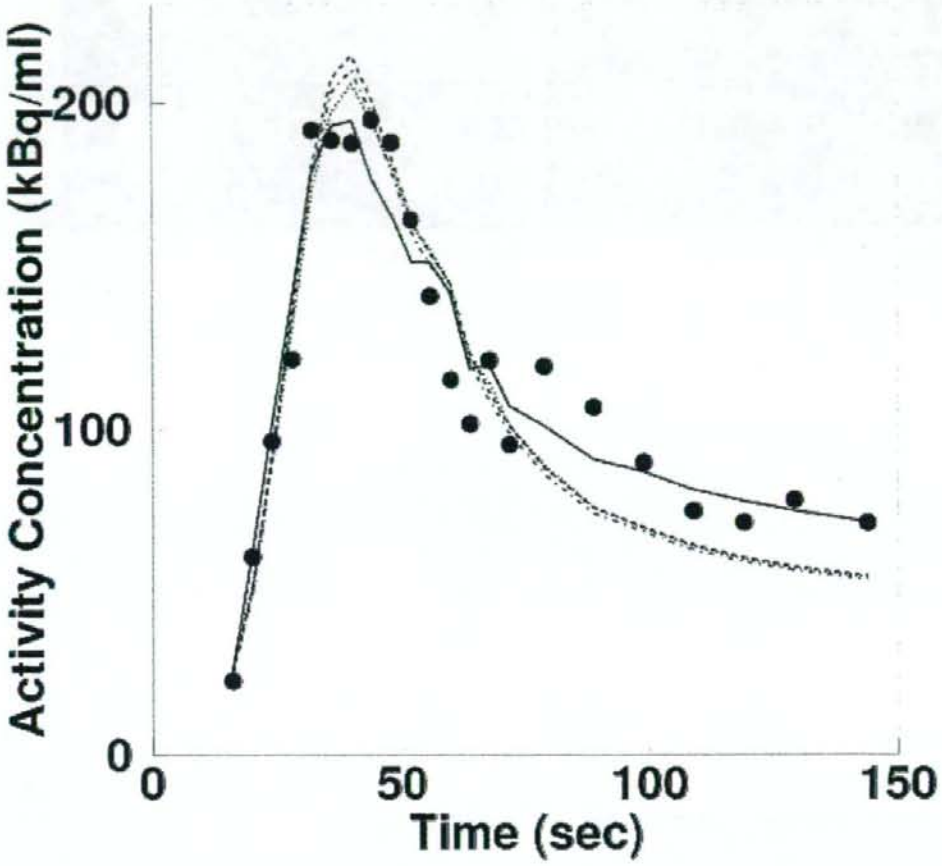

Figure 4

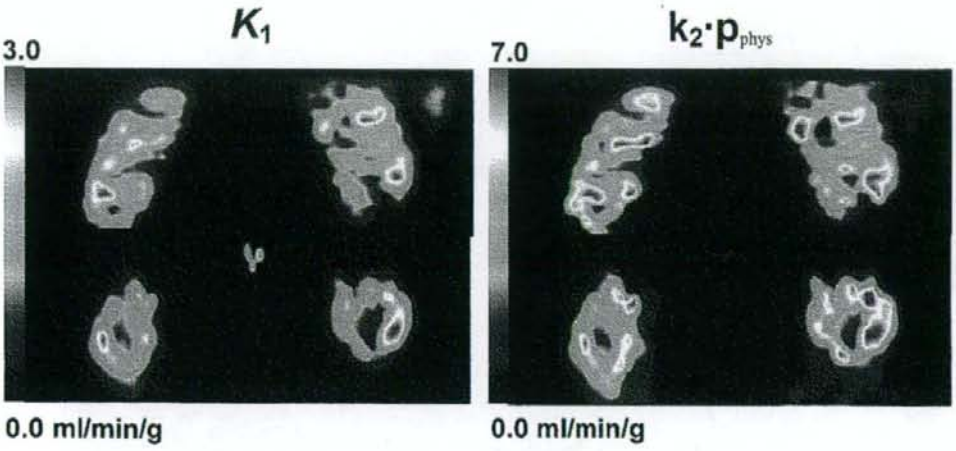

Figure 5

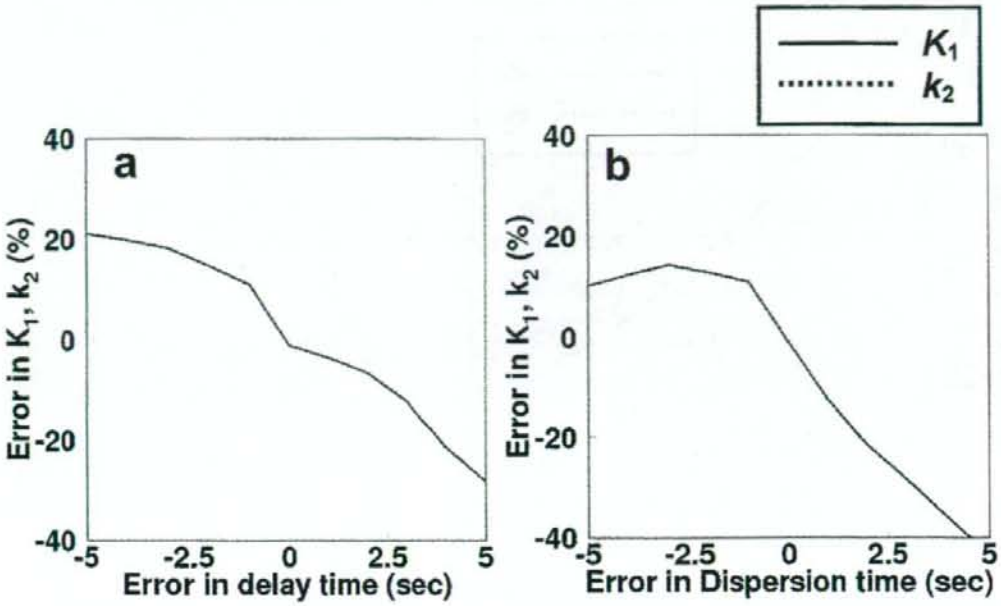
K_1
k_2
a
b
40
20
0
-20
-40
Error in K_1, k_2 (%)
-5
-2.5
0
2.5
5
Error in delay time (sec)
Error in Dispersion time (sec)

Figure 6